PROCEEDINGS, Thirty-Seventh Workshop on Geothermal Reservoir Engineering
Stanford University, Stanford, California, 30 Jan 2011-1 Feb 2012

THE EFFECT OF THERMOELASTIC STRESS CHANGE IN THE NEAR WELLBORE REGION ON HYDRAULIC FRACTURE GROWTH

Rob Jeffrey, Bisheng Wu and Xi Zhang

CSIRO Earth Science and Resource Engineering
Ian Wark Laboratory
Melbourne, Victoria, 3168, Australia,
Rob.Jeffrey@csiro.au

ABSTRACT

The effect of cooling the rock mass near the wellbore on hydraulic fracture growth is considered by use of 2D plane strain numerical models. The thermoelastic stress change after 5 days of cooling while holding the wellbore at 100 ^{0}C cooler than the reservoir temperature is first calculated using a thermoelastic wellbore model. The thermoelastic stress change is then combined with the far-field stresses and applied to different wellbore and natural fracture configurations in the hydraulic fracturing model. The fracturing model then calculates the pressure, opening, shearing, length and fracture path. Cooling is found to reduce the fracturing pressure, result in fractures that open wider and are correspondingly shorter than they are when grown without cooling. Restrictions along the fracture path, such as offsets, are opened more widely after cooling which reduces the pressure required to force fluid through them and because of this, in some cases the hydraulic fracture will grow to be more symmetric in length with respect to the wellbore for the cooled rock conditions.

INTRODUCTION

During stimulation and production of a geothermal reservoir, a number of types of coupled processes between the fluid and the rock take place. The effect of the coupling of temperature and pressure change with elastic deformation has been studied by many researchers (e.g. see Abe et al., 1979; Shibuya et al., 1985; Ghassemi et al., 2008). This paper considers the affect of stress changes in the near-wellbore region on hydraulic fracture growth.

Wellbore cooling has been previously considered as a method to generate fractures and increase the permeability of existing fractures in geothermal reservoirs (Duda, 1985; Perkins and Gonzalez, 1985). In this paper we consider a set of problems that involve near-wellbore fracture deformation associated with propagation of an opening mode hydraulic fracture. We include the wellbore as part of the problem and compare hydraulic fracture growth for cases with and without cooling of the near-wellbore region. One case considered includes interaction of the hydraulic fracture with pre-existing natural fractures.

MOTIVATION FOR PROBLEMS STUDIED

Hydraulic fractures are typically modeled as planar features and any surface roughness is lumped into a friction factor incorporated into the fluid flow solution. However, it has been recognized for some time that when hydraulic fractures interact with natural fractures, offsets and fracture branches are often formed (Warpinski and Teufel, 1987) and the presence of these is now recognized to have a significant impact on fracture pressure and growth rate (Daneshi, 2007; Jeffrey et al., 2009a).

Fig. 1 contains a photograph of a hydraulic fracture propped with yellow plastic proppant and illustrates a case where the hydraulic fracture has developed offsets during its crossing interaction with natural fractures. This fracture was placed at 580 m depth into a naturally fractured orebody consisting of monzonite porphyry and volcanic sediments, which in stiffness and strength are similar to deeper granitic geothermal reservoir rocks. The trace of the hydraulic fracture has been enhanced in this photograph, but its path is clearly visible in the un-retouched photo when enlarged.

Offsetting of the hydraulic fracture channel, as illustrated in Fig. 1, has been documented by nearly all mine through mapping exercises and was a primary feature of all five fractures mapped at the Northparkes E48 site (Jeffrey et al., 2009b). Numerical modeling of one such fracture that contained a large offset along a shear zone was described by Jeffrey et al. (2010), and that paper focused on the interaction of the hydraulic fracture

with the shear zone, without thermoelastic effects. It is expected that hydraulic fractures grown from a geothermal well will interact in similar ways with the fractured reservoir rock. This paper therefore deals with that problem and specifically studies the effect that cooling of the near-well rock might have on fracture growth.

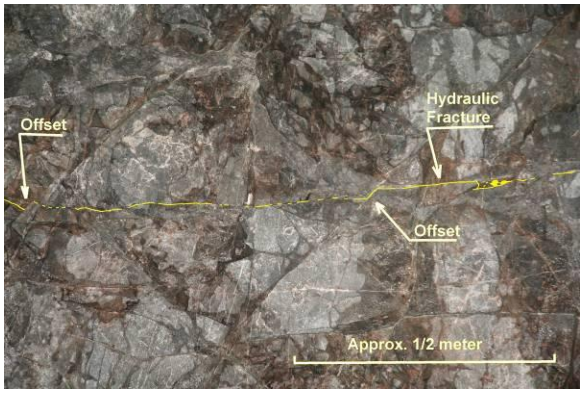

Figure 1: Photograph during mining of fracture 7 at the Northparkes E48 site. See Jeffrey et al., (2009b) for details.

PROBLEM FORMULATION

The geometries of the problems considered in this paper are contained in Fig. 2, which shows the cross section of a well whose axis coincides with the maximum or intermediated in situ principal stress. The wellbore is assumed to be long enough that the fracturing process can be regarded as a plane strain type problem. The in-plane coordinate system is also shown in Fig. 2. The wellbore radius is denoted as r_w . The initial fracture shapes and sizes are given based on predefined paths. In particular, the direction of initial hydraulic fractures from the wellbore is also defined. The pre-existing natural fractures are given a small conductivity for fluid flow to simulate the effects of asperities or partial mineralization along the fracture surface.

Prior to fracturing, the system is in an equilibrium state under a temperature distribution generated by cooling. The cooling occurs under the conditions of the initial formation temperature T_R^* and a fixed wellbore temperature T_w^* (less than T_R^*). The wellbore cooling is assumed to last for a given time (5 days in this paper) so that a nearly steady stress state is reached. Under the cooling induced non-uniform temperature field, the near-well stress fields are altered too, thus affecting the fracture permeability and subsequent fracture paths.

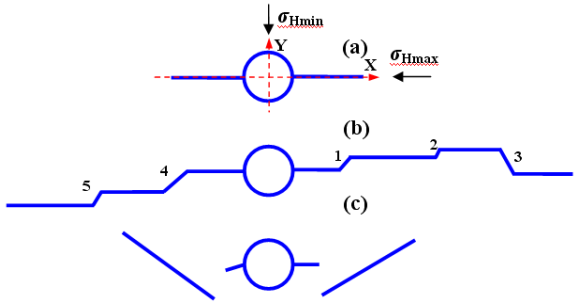

Figure 2: Geometry models for case studies. (a) A bi-wing planar fracture, (b) Predefined path with offsets, (c) Interaction with natural fractures.

The basic governing equations and the boundary conditions are described in our previous work (Zhang et al., 2009, 2008), that deal with fully coupled mechanisms of rock deformation and fluid flow. The basis of the hydraulic fracture model is described next.

1. Fluid volumetric flux q in a closed fracture segment is described by

$$q = -\frac{\varpi^3}{\mu'}\frac{\partial p_f}{\partial s} \tag{1}$$

and in an opened fracture portion it is

$$q = -\frac{(w+\varpi)^3}{\mu'}\frac{\partial p_f}{\partial s} \tag{2}$$

where $\mu' = 12\mu$ with μ being fluid dynamic viscosity, w and ϖ are mechanical opening and initial hydraulic aperture and the latter does not cause any stress change. The hydraulic aperture is assigned to fractures to establish their hydraulic conductivity when closed p_f is the fluid pressure.

2. Fluid flow in the opened fracture portion is based on the lubrication equation:

$$\frac{\partial(w+\varpi)}{\partial t} = \frac{\partial}{\partial s}\left(\frac{(w+\varpi)^3}{12\mu}\frac{\partial p_f}{\partial s}\right) \tag{3}$$

but fluid flow in the closed fracture segment is based on the pressure diffusion equation

$$\frac{\partial p_f}{\partial t} - \frac{1}{\chi_1\mu'}\frac{\partial}{\partial s}(\varpi^2\frac{\partial p_f}{\partial s}) = 0 \tag{4}$$

where χ_1 is the compressibility of the fracture with units Pa^{-1}. It is set as 10^{-8}/Pa in the paper.

3. The nonlocal elastic equilibrium equations for multiple fractures are given as:

$$\sigma_n(\boldsymbol{x},t)-\sigma_1(\boldsymbol{x})=\sum_{r=1}^{N}\int_0^{l_r}[G_{11}(\boldsymbol{x},s)w(s,t)+G_{12}(\boldsymbol{x},s)v(s,t)]ds$$
$$\tau_s(\boldsymbol{x},t)-\tau_1(\boldsymbol{x})=\sum_{r=1}^{N}\int_0^{l_r}[G_{21}(\boldsymbol{x},s)w(s,t)+G_{22}(\boldsymbol{x},s)v(s,t)]ds \quad (5)$$

where $\boldsymbol{x}$=(x,y), t is time and v is the shear displacement discontinuity. l_r is the length of fracture r. σ_n is the normal stress and τ_s is the shear stress arising from frictional sliding and obeying Coulomb's frictional law characterized by the coefficient of friction λ, such that $|\tau_s| \le \lambda\sigma_n$, in parts of fractures that are in contact. Along the opened fracture portions, we have $\sigma_n=p_f$.

In addition, σ_1 and τ_1 are the normal and shear stresses, respectively, along the fracture direction at location x caused by the far-field stresses and thermal effects.

G_{ij} are the hypersingular Green's functions, which give the stress components at location $\boldsymbol{x}$ caused by a unit displacement discontinuity along the fracture at a distance s. They are directly proportional to the plane strain Young's modulus.

4. The global mass balance must satisfy

$$\sum\int_0^{l_f}(w+\varpi)ds=Q_0t \quad (6)$$

5. And the fluid front in the fracture will, in general, not coincide with the fracture tip. The fluid font moving speed is defined by

$$\dot{l}_f=q(l_f,t)/w(l_f,t) \quad (7)$$

6. The fracture growth criterion (Erdogan and Sih, 1963) is

$$\cos\frac{\Theta}{2}(K_I\cos^2\frac{\Theta}{2}-\frac{3}{2}K_{II}\sin\Theta)=K_c \quad (8)$$

where K_I and K_{II} are calculated stress intensity factors. K_c is fracture toughness and Θ is the fracture propagation direction relative to the current fracture tip orientation.

The problems must be closed by the imposed boundary conditions at the wellbore, that is, the sum of injection rates to each hydraulic fractures must equal the given total injection rate Q_0, and at the fracture tip the displacement discontinuities are both zero, $w(\ell_r,t)=0$ and $v(\ell_r,t)=0$

The numerical scheme for solving the above nonlinear and nonlocal coupling problem with moving boundaries has been detailed in our previous work (Zhang et al., 2005) based on the Displacement Discontinuity Based Boundary Element Method. The wellbore, the hydraulic fractures, and any natural fractures are discretised with constant displacement elements. The rigid motion caused by the introduction of the wellbore can be eliminated as discussed in Zhang et al. (2011). The model has been applied to solving hydraulic fracturing problems with viscous fluid flow and the solutions are consistent with existing results with and without coupling. In addition, crack propagation is triggered when the opening and width solutions satisfy the propagation criterion.

In this paper, the thermal stresses around the wellbore are first obtained using the thermoelastic model proposed by Wu et al. (2011) without any far-field stresses acting. The thermal-induced stress change is then treated as constant during the period of fracture growth because the fracturing time is not long enough for significant heat diffusion and fluid-rock heat exchange to occur. Therefore, the thermal stress can be treated in the same manner as confining stresses that are induced by far-field stresses and this thermal decoupling is considered as a good approximation for the short-duration fracturing process studied here. It should be noted that the thermal effect on material properties is not taken into account in this paper.

Table 1: Parameters for the calculation of the thermal stress and for the hydraulic fracture simulation

Young modulus E (MPa)	50000
Poisson ratio v	0.2
Fluid viscosity (Pa·s)	0.04
Fracture toughness K_c (MPa·m$^{1/2}$)	1.35
Injection rate Q_0 (m^2/s)	0.0001
Max horizontal principal stress σ_{Hmax} (MPa)	80
Min horizontal principal stress σ_{Hmin} (MPa)	50
Formation temperature T_R^* (^{0}C)	250
Wellbore temperature T_w^* (^{0}C)	150
Wellbore radius r_w (m)	0.1
Coefficient of friction λ	0.6
Thermal expansion coefficient (1/K)	5×10^{-5}

Table 2: Geometry of offsets for Case (b)

Offset Number	1	2	3	4	5
Angle (deg)	45	60	300	225	240
Length (m)	0.1	0.02	0.15	0.15	0.08

STUDY CASES

The three different geometry configurations, as shown in Fig. 2, will be considered in this section. All the mechanical properties and other parameters are as listed in Table 1, unless otherwise specified. The crack initiation and propagation are affected by near-well stress fields, which depend on the wellbore size, crack orientation angle, initial crack length, far-

field stresses, and also on the thermal stress. Here we focus on the difference in fracturing behavior with and without the presence of thermal stress.

Case (a)

For the straight planar fracture as shown in Fig. 2(a), it is assumed that there initially exists a bi-wing fracture with each wing having a length of 0.36 m and an opening of 0.01 mm. As the fracture shape and far-field stresses are symmetrical, the normal (closure) stresses acting on the surface of the two fractures are identical and the shear stresses acting on the fracture surface are zero. The magnitude of σ_y acting on along the x-axis is plotted in Fig. 3 for CT=0 and CT=5 (CT stands for cooling time and the time is in days.), illustrating the stress change along the path of a planar fracture. Fig. 4 compares the mechanical opening, fluid pressure, fracture length and injection pressure at several times under different cooling conditions for such a planar fracture. The red curves are for the case without cooling effects, i.e. CT=0 and the blue ones for the case CT=5 (days) with the wellbore held at 100 ^{o}C cooler than the reservoir for the entire time. With the fracturing fluid injected into the well at a constant rate, the fracture opening increases as shown in Fig. 4(a).

Compared with the case CT=0, the thermal cooling reduces the injection pressure as evident from the results in Figs. 4(b) and (c). For CT=5 days, the induced thermal stress decreases the tangential stresses near the wellbore and when combined with the far-field stress, the total compressive stress acting on the plane of the fracture path is decreased. The stress change is greatest at the wellbore, which results in a non-uniform closure stress along the fracture path. This directly leads to the increase in the fracture opening and an associated reduction in fluid pressure compared to the case without cooling. Moreover, the injection pressure trend is different for the two cases. For CT=0, the injection pressure reaches a maximum value quickly and then decreases slowly in time, as is considered normal for conventional plane strain models of hydraulic fracturing treatments. However, the injection pressure for the cooled wellbore conditions shows a monotonic increase with time.

The fracture lengths in the presence and absence of cooling are compared in Fig. 4(*d*). It can be seen that the fracture growth is reduced significantly after cooling occurs (e.g. see Fig. 5). Because the injected volume of fluid is the same for both cases, the wider fracture growing in cooled rock must then be shorter at any given time.

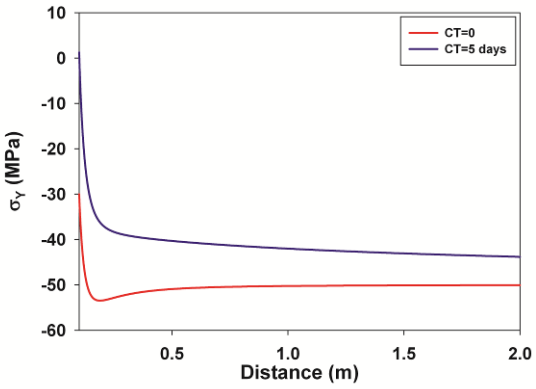

Figure 3: Variation of σ_y along the x axis. Compressive stress is negative.

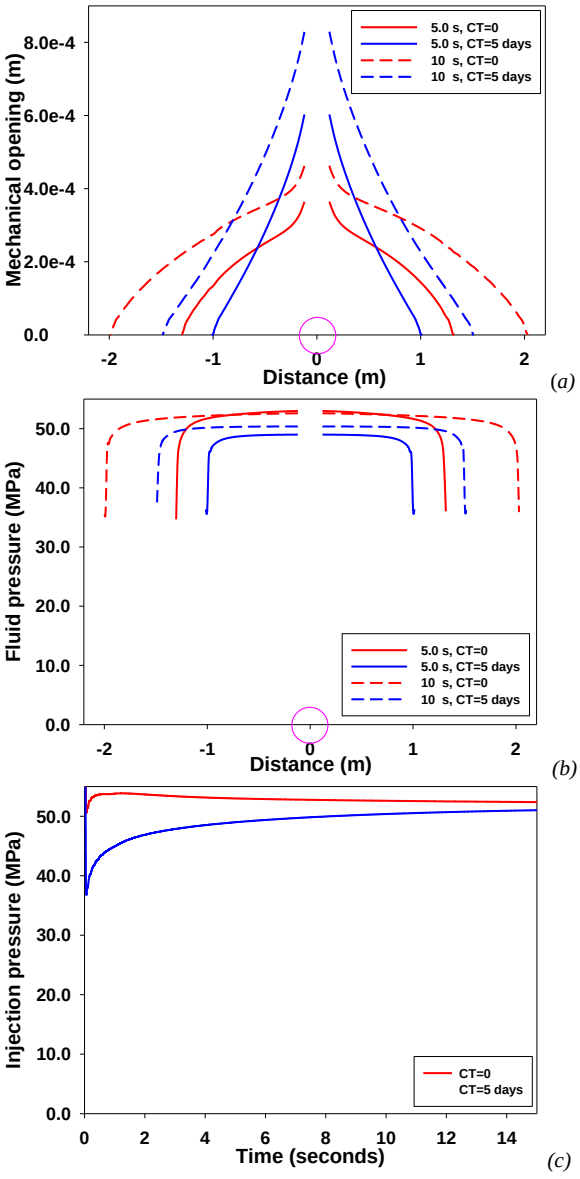

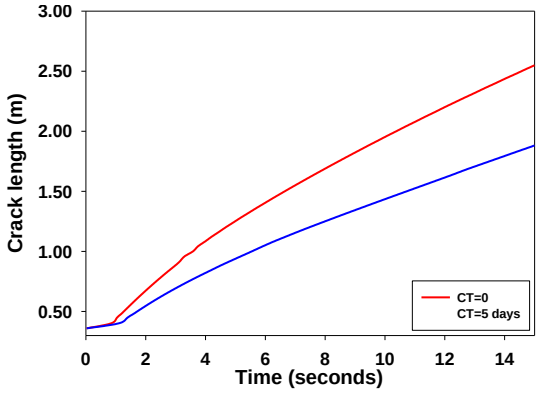

(*d*)

Figure 4: (a) opening displacement, (b) pressure distribution, (c) injection pressure and (d) crack length with time for Case (a).

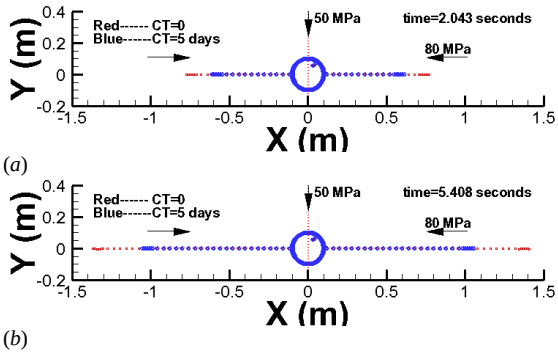

(*a*)

(*b*)

Figure 5: Fracture growth paths for Case (a).

Case (b)

Next we consider growth of fractures with offsets along their paths. To start, we predefine the path so the fracture grows with the same geometry for both the uncooled and cooled rock conditions. The offsets develop at locations where an interaction occurs with an existing joint, natural fracture or fault (Warpinski and Teufel, 1987; Jeffrey et al., 2009a). Detailed descriptions of each offset are given in Table 2. The offsets on the right side of the wellbore are assigned a small initial hydraulic conductivity (w_0 =0.01 mm) while the offsets to the left of the wellbore are assigned a larger initial conductivity (w_0 =0.05 mm). The assigned fracture conductivity allows some fluid to pass through portions of the fracture, such as at offsets that are closed. The horizontal step sizes from the left to the right are all 0.25 m except for the fifth offset, which is 0.4 m. Fig. 6(a) gives the comparison of the mechanical opening responses with and without cooling effects. Distance is measured from the wellbore center along a straight line parallel to the x-axis. As discussed above, the thermal-induced reduction in compressive stress is significant along the path of the hydraulic fracture. The near-well opening is significantly larger at CT=5 days than it is for the case CT=0. However, the offsets play a role in restricting fluid flow and limiting opening downstream of them for both cases. The lower fluid pressure associated with fracturing the cooled rock affects the movement of fluid in the hydraulic fracture. The offsets are narrow and are subject to relatively high confining stress. For the fracture geometry studied, the opened fracture length on the right-hand side of the wellbore (RHS) is significantly shorter compared to a straight fracture for cooling as considered in case CT=5 days.

The existence of offsets can induce slip not only on the offsets, but also on the steps. The kinematic deformation transfer between the offset and the step is considered as an important factor for fracture opening development (Jeffrey et al., 2010). The increase of the opening at each offset intersection point is attributed to this transfer as shown in Fig. 6(a) at offset 4 (first offset on the left side of the wellbore) for CT=0.

The pressure loss across offset 1 is initially relatively large as shown in Fig. 6(c). This loss is nearly completely removed at t=2.5s for CT=0 days, but a measureable loss still exists at t=2.5s for the CT=5 days case. In contrast, the pressure distribution is more uniform at later times on the left-hand side (LHS) for both cases. As the fracture grows and opens the offsets, the fracture width across the offset can open sufficiently to eliminate the width-induced pressure drop there. The unopened offsets farther from the wellbore then become the main sites for significant pressure losses in the growing fracture. A 3D fracture model with offsets would allow more freedom for the fluid to move around an offset and would be expected to display less extreme pressures and opening responses, but the overall trends would be similar.

The cooling-induced injection pressure reduction is clear in Fig. 6(d). Depending on the details of offsets encountered, the fracture length may develop differently, leading to asymmetric fracture penetration into the rock mass.

Now we turn to a problem related to Case (b), namely hydraulic fracturing growth across existing geological discontinuities. This type of growth is the primary process that generates offsets along a hydraulic fracture path. We will consider here the detail of how such offsets arise from such interactions.

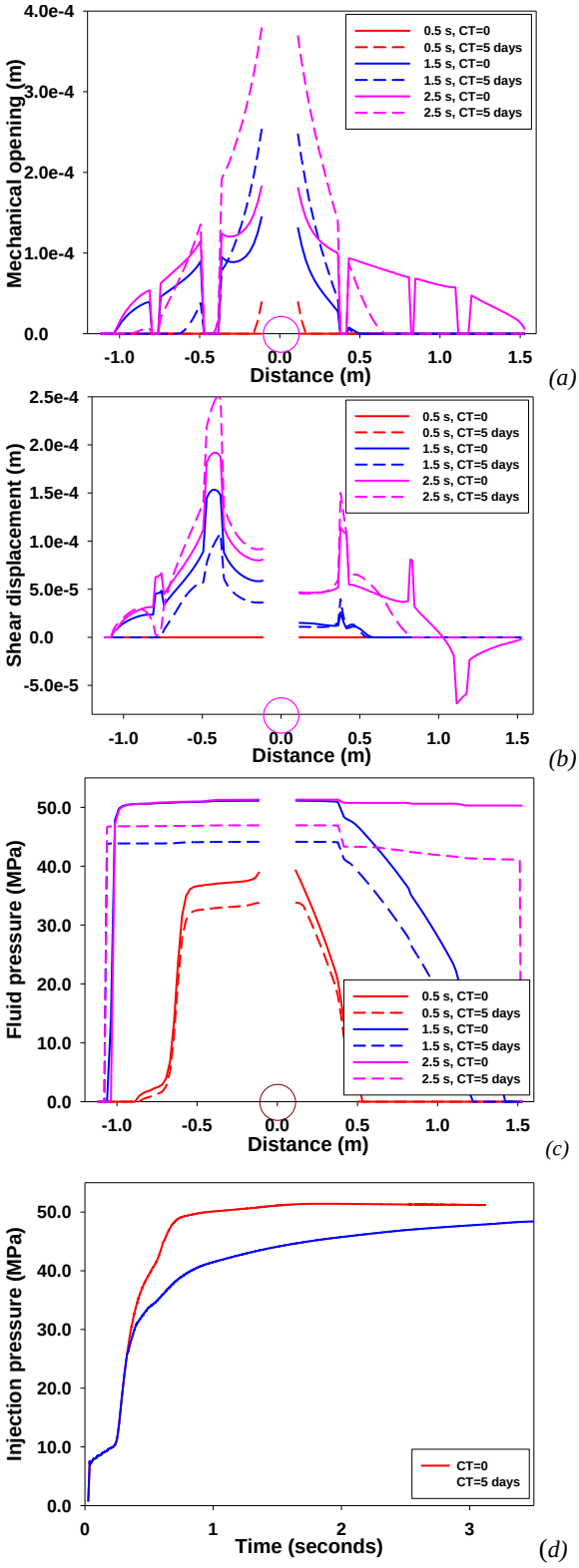

Figure 6: (a) opening displacement, (b) shear displacement, (c) pressure distribution and (d) injection pressure with time for Case (b)

Case (c)

Four different geometric arrangements of pre-existing fractures will be considered (referred to as case (c1) to case (c4). The case (c1) is a symmetric case in which the hydraulic fracture grows from wellbore in the σ_{Hmax} direction and the natural fractures are both at angles of 30º with respect to *x* axis. Case (c2) considers the same geometry as case (c1) except that the initial LHS flaw at the wellbore wall is inclined at an angle of 20º, instead of 0º with respect to *x* axis. Case (c3) is based on the arrangement of Case (c2), but the left-hand side natural fracture is twice as long as the right-hand side one. Case (c4) is based on case (3), but reversing the lengths of the right and left hand side natural fracture sizes.

Fig. 7 displays the symmetric fracture path development for case (c1). The paths for CT=0 and 5 days follow each other. The lengths of the red (CT=0) and blue (CT=5 days) bars perpendicular to the fracture path indicate the fluid pressure magnitude and distribution. Results for this case again show that the fracture length is shorter after cooling at the same time because of the larger fracture opening for the cooled case. Also, as the pre-existing fractures are not aligned with the maximum stress direction, there is a rotation in the hydraulic fracture path as the fracture seeks to propagate in the direction with least resistance as shown in the *t*=1.95 second plot in the lower part of Fig. 7.

Compared with the symmetric case shown in Fig. 7, a small perturbation on fracture geometry can produce significant deviation in path direction and length for either the left or right fractures. This is because the any restriction to growth leads to more growth on the other side, increasing the asymmetry.

Fig. 8 shows fracture path and pressure distributions for case c2 where the left flaw at the wellbore is oriented at 20º with respect to the x-axis. The red path in Fig. 8 indicates the right side fracture grows preferentially, when no cooling occurs. However, this effect is minimized by the cooling. The blue path shows that the right and left fracture lengths are roughly equal after cooling of the rock because the reduction of near-well stress caused by cooling promotes addition opening and removes the restriction associated with the misaligned flaw on the left side.

This analysis is supported by the pressure and normal stress variations shown in Fig. 9. Along opened portions of the hydraulic fracture, the pressure is equal the normal stress and in closed portions the pressure is less than the normal stress. The curves in Fig. 9 start from one end of the natural fracture and end at the fracture tip. It is clear that under CT=0, the

left fracture is fully closed and the pressure level is much lower than its RHS counterpart. This is caused by the higher pressure needed to open the left flaw which is subject to higher normal stress. The right side fracture extends before the pressure reaches a high enough value to open the left flaw. For long-term cooling, the reduced stress field results in a smaller normal stress acting on the left flaw and both are opened and extended. The normal stresses acting on the left and right flaws are approximately equal as can be seen by the dashed blue lines in Fig. 9. Also, entry of the hydraulic fracture into the natural fractures on either side of the wellbore occurs equally, allowing more symmetric fracture growth into and past these natural fractures.

The geometry configuration for cases c3 and c4 consider the effect of varying the natural fracture lengths on either side of the wellbore. Figs. 10 and 11 contain growth and pressure results. It is interesting to note that under CT=0, the fracture tortuosity of the LHS starter fracture plays a strong role in generating a pressure drop that inhibits growth on that side and causes the RHS fracture to propagate faster, independent of the natural fracture length. However this situation is changed when the long-term cooling is introduced. It is found that the ultimate hydraulic fracture length depends on the initial natural fracture length. As the near well pressure loss is not significant, the difference seems to arise because of the higher pressure required to open the natural fracture (because of its orientation).

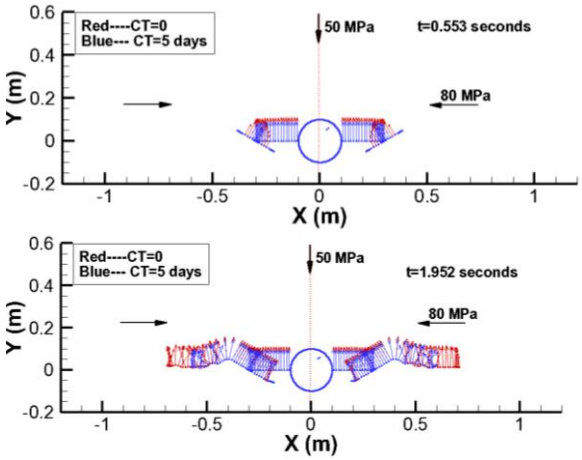

Figure 7: Fracture growth path for Case c1. The initial cracks are symmetric about x=0.

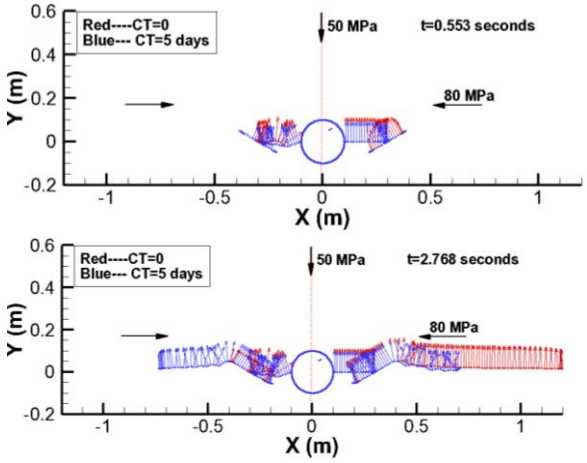

Figure 8: Fracture growth for Case c2. The initial left flaw is 20° inclined with x axis compared with Case c1.

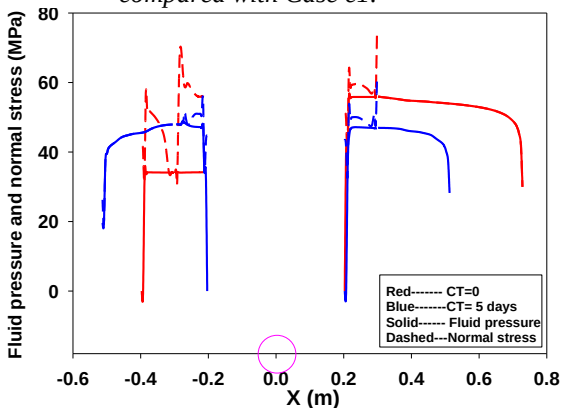

Figure 9: Variation of pressure and normal stress along the x axis at t=1.5 seconds.

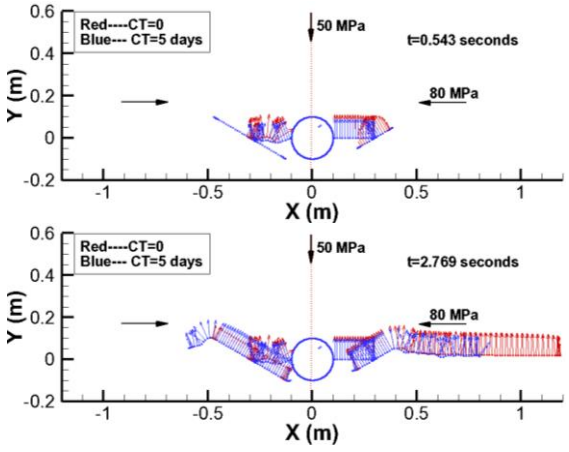

Figure 10: Fracture growth for Case c3. The length of the initial left natural fracture is twice that of the right one compared with Fig.5.

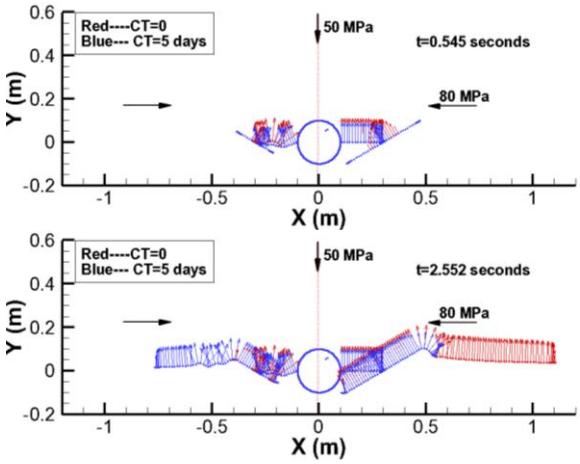

Figure 11: Fracture growth for Case c4. The length of the initial right natural fracture is twice that of the left one compared with Fig.7.

The longer the pre-existing fracture, the larger the pressure drop. However, for the cases considered, new fracture initiation still occurs from both the short and longer natural fractures, but the overall hydraulic fracture length is larger on the side of the shorter natural fracture.

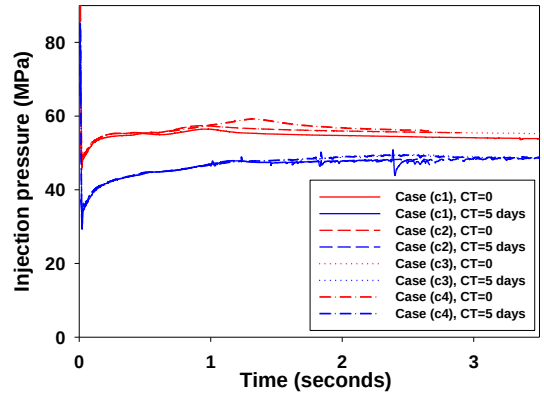

Figure 12: Injection pressure for above Case (c1) to Case (c4).

The time-dependent injection pressures for the four geometry configurations are plotted in Fig. 12 under CT=0 and 5 days. The injection pressure does not change much for different geometrical configurations but is dependent on whether cooling has occurred or not. However, there is a considerable change in fracture path. Therefore a small perturbation can cause fluid flow and fracture growth in a preferential direction. This change in path is a result of the hydraulic fracture seeking to minimize the energy required to propagate and makes no significant difference in fluid power.

CONCLUSIONS

This paper considers the growth of a hydraulic fracture from a wellbore under conditions where the wellbore either is or is not first subject to cooling. Planar and offset hydraulic fracture growth has been studied. From this study we draw the following conclusions:

Cooling of the near-wellbore rock will reduce the stress acting across hydraulic fractures growing in this region, leading to fractures that open more widely and grow more slowly for conditions where the injection rate is constant.

When the hydraulic fractures grow along non-planar paths the interaction with natural fractures or offsets near the well can lead to one wing extending further than the other. This asymmetry is reduced by cooling the well as the thermoelastic stress change allows the offset or natural fracture to open more, removing the restriction to fluid flow that produces the asymmetry.

ACKNOWLEDGEMENTS

The authors thank CSIRO for supporting the work described here and granting permission to publish this paper.

REFERENCES

Abe, H., Keer, L., and Mura, T. (1979), Theoretical study of hydraulically fractured penny-shaped cracks in hot, dry rocks, *International Journal for Numerical and Analytical Methods in Geomechanics*, *3*(1), 79–96. Wiley Online Library.

Daneshy, A. (2007), Pressure variations inside the hydraulic fracture and their impact on fracture propagation, Conductivity, and Screenout. *SPE Production & Operations*, *22*(1). doi:10.2118 /95355-PA

Duda, L.E. (1985), Investigation of wellbore cooling by circulation and fluid penetration into the formation using a wellbore thermal simulator computer code, International Symposium on Geothermal Energy, Kailua Kona, HI, USA, August 26.

Erdogan, F. and Sih, G.C. (1963), On the crack extension in plates under plate loading and transverse shear, J. Basic Eng., Vol. 85, pp. 519-527.

Ghassemi, A., Nygren, A., and Cheng, A. H.-D. (2008), Effects of heat extraction on fracture aperture: A poro–thermoelastic analysis. *Geothermics*, *37*(5), 525-539. doi:10.1016 /j.geothermics.2008.06.001

Jeffrey, R., Bunger, A., Lecampion, B., Zhang, X., Chen, Z., van As, A., Allison, D., et al. (2009b), Measuring hydraulic fracture growth in naturally fractured rock, *SPE Annual Technical Conference and Exhibition* (pp. 1-18).

Jeffrey, R.G, Zhang, X. and Bunger, A.P. (2010), Hydraulic fracturing of naturally fractured reservoirs, Thirty-Fifth Workshop on Geothermal Reservoir Engineering, Stanford University, Stanford, California, USA, February 1-3.

Jeffrey, R., Zhang, X., and Thiercelin, M. (2009a), Hydraulic fracture offsetting in naturally fractured reservoirs: quantifying a long-recognized process, *Proceedings of SPE Hydraulic Fracturing Technology Conference*. Society of Petroleum Engineers. doi:10.2118 /119351-MS

Perkins, T.K. and Gonzalez, J.A. (1985), The effect of thermoelastic stresses on injection well fracturing, Society of Petroleum Engineers Journal, 78-88.

Shibuya, Y., Sekine, H., Takahashi, Y., and Abe, H. (1985), Multiple artificial geothermal cracks in a hot dry rock mass for extraction of heat, *Journal of Energy Resources Technology*, *107*, 274.

Warpinski, N., and Teufel, L. (1987), Influence of geologic discontinuities on hydraulic fracture propagation, *Journal of Petroleum Technology*, (February), 209-220.

Wu, B., Zhang, X. and Jeffrey, R.G. and Wu, B. (2011), A semi-analytic solution of a wellbore in a non-isothermal low-permeability porous medium under non-hydrostatic stresses, International Journal of Solids and Structures, under review.

Zhang, X. and Jeffrey, R.G. (2008), Reinitiation or termination of fluid-driven fractures at frictional bedding interfaces, *Journal of Geophysical Research*, Vol. 113, B08416.

Zhang, X., Jeffrey, R.G, Bunger, A.P. and Thiercelin, M. (2011), Initiation and growth of a hydraulic fracture from a circular wellbore, International Journal of Rock Mechanics & Mining Science, Vol.48, pp. 984-995.

Zhang, X., Jeffrey, R.G. and Detournay, E. (2005), Propagation of a fluid-driven fracture parallel to the free surface of an elastic half plane, International Journal for Numerical and Analytical Methods in Geomechanics, Vol.29, pp. 1317–1340.

Zhang, X., Jeffrey, R.G and Thiercelin, M. (2009), .Mechanics of fluid-driven fracture growth in naturally fractured reservoirs with simple network geometries, Journal of Geophysical Research, Vol.114, B12406.